

Conditional Generation Scheme for a High-fidelity Yurke-Stoler States by Mixing Two Coherent Beams with Squeezed Vacuum State

Sun-Hyun Youn*

Department of Physics, Chonnam National University, Gwangju 500-757, Korea

Abstract

The numerical conditions to generate a high-fidelity Yurke-Stoler states ($|\alpha > + e^{i\psi} | -\alpha >$) were found for two cascade-placed beam splitters with one squeezed state input and two coherent state inputs. Controlling the amplitude and the phases of beams, allows for various Yurke-Stoler states to be manipulated with ultra high-fidelity, and the expected theoretical fidelity is of more than 0.9999.

PACS numbers: 42.25.-p, 03.65.-w, 42.50. Lc

Keywords: Nonclassical light, squeezed state, Schrodinger Cat state, Yurke-Stoler state, photonic state engineering

arXiv:1410.1398v2 [physics.optics] 23 Nov 2014

* email: sunyoun@chonnam.ac.kr, fax: +82-62-530-3369

I. INTRODUCTION

The generation of specific quantum states at a high-fidelity plays an essential role in quantum information science[1, 2]. Manipulating nonclassical light that is originally generated by a nonlinear interaction between the light fields and the medium has been an effective method for engineering the desired non-classical photonic state in a quantum process[2, 3].

The manipulation of the nonclassical state usually adopts a conditional state-preparation scheme that takes advantage of a strong nonlinearity induced by the quantum measurement, even at the level of a single photon. By measuring one of the entangled photons produced in the parametric down conversion, the arbitrary superposition of vacuum and single-photon states has been accomplished[4] and a variant combination of coherent states and Fock states are conditionally created and analyzed [5–9].

Generating nonlinear photonic-states, such as Schrodinger states, using a squeezed light source by means of conditional measurements on a beam splitter has also been extensively studied, both theoretically and experimentally[10–14].

In our proposed system, the junction of the field coherent state is added to the non classical state [15], and the photon is subtracted from the squeezed vacuum[16]. We added two coherent beams with cascade placed beam splitters, as seen in Fig. 1. The two beamsplitters and two coherent beams give us a degree of freedom to control the output in a highly nonclassical manner. We characterize the single output from the three input beams with a simultaneous detection of two photo detectors. Our system has a great advantage in that it can generate a high-fidelity Fock-state [17, 18].

In this article, we study the condition to generate high-fidelity Yurke-Stoler state ($|\alpha > +e^{i\psi} | -\alpha >)$ [19]. The well-known Schrodinger-cat states are a special case of the Yurke-Stoler state, and recently, the Schrodinger-cat state has been generated from classical radiation in the microwave region through a subtraction measurement [20], and a macroscopic Schrodinger-cat state has been generated in a nanomechanical resonator [21]. Basically two targets have been set to generate a Schrodinger-cat state. The first one is to obtain a giant Schrodinger cat state (high α), and the second is to generate a high-fidelity one.

The present paper is organized as follows. In Section II, we introduce our system with two cascade placed beam splitters, with one squeezed state and two coherent state inputs.

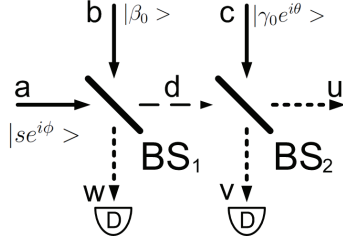


FIG. 1: Schematic diagram of the Yurke-Stoler state generation. One squeezed state is in the input mode a ($|se^{i\phi}\rangle$), and two coherent states ($|\beta_0 = 0\rangle, |\gamma_0 e^{i\theta}\rangle$) are in the input modes b , and c . BS: Beam Splitter. D: Detector.

In Section III, we explicitly calculate the probability of the amplitude when two detectors at the output port simultaneously detects a single photon, and then we find the condition for which the output port generates a high-fidelity Yurke-Stoler state in Section IV. To obtain an optimal state, we tested the square of the Wigner function differences, which are more sensitive than the fidelity. In Section V, we summarize the main results and discuss the experimental implementation.

II. TWO CASCADE PLACED BEAM SPLITTERS

Let a squeezed vacuum state $|\xi\rangle$ be in the input mode a , and the two coherent states, $|\beta\rangle$ and $|\gamma\rangle$, be in the input modes b and c , as seen in the experimental set up in Fig. 1. Then, the input state $|\xi\rangle, |\beta\rangle, |\gamma\rangle$ can be expressed in the number-state representation [22]:

$$|\xi, \beta, \gamma\rangle = e^{-\frac{1}{2}(|\beta|^2 + |\gamma|^2)} \sum_{n_\xi=0, n_\beta=0, n_\gamma=0} C_{n_\xi} \frac{\beta^{n_\beta}}{\sqrt{n_\beta!}} \frac{\gamma^{n_\gamma}}{\sqrt{n_\gamma!}} |n_\xi\rangle_a |n_\beta\rangle_b |n_\gamma\rangle_c, \quad (1)$$

where C_{n_ξ} is the coefficient of the squeezed vacuum with squeezing parameter, $se^{i\phi}$, and is zero for all odd values of n_ξ and nonzero only for an even value of n_ξ . The nonzero values

of C_{n_ξ} for even values of n_ξ become [22]:

$$C_{n_\xi} = \frac{\sqrt{n_\xi!}}{\sqrt{\cosh s \frac{n_\xi}{2}!}} \left(-\frac{1}{2} e^{i\phi} \tanh s\right)^{\frac{n_\xi}{2}}. \quad (2)$$

With the experimental set up in Fig. 1, the three creation operators $\hat{a}^\dagger, \hat{b}^\dagger, \hat{c}^\dagger$ are written in terms of three creation operators $\hat{w}^\dagger, \hat{v}^\dagger, \hat{u}^\dagger$. Using the operator relation [23], we can obtain the relations between the input modes and the output modes as the following,

$$\begin{pmatrix} \hat{a}^\dagger \\ \hat{b}^\dagger \end{pmatrix} = \begin{pmatrix} t_1 e^{-i\phi_{\tau_1}} & \sqrt{1-t_1^2} e^{-i\phi_{\rho_1}} \\ -\sqrt{1-t_1^2} e^{i\phi_{\rho_1}} & t_1 e^{i\phi_{\tau_1}} \end{pmatrix} \begin{pmatrix} \hat{d}^\dagger \\ \hat{w}^\dagger \end{pmatrix} \quad (3)$$

$$\begin{pmatrix} \hat{d}^\dagger \\ \hat{c}^\dagger \end{pmatrix} = \begin{pmatrix} t_2 e^{-i\phi_{\tau_2}} & \sqrt{1-t_2^2} e^{-i\phi_{\rho_2}} \\ -\sqrt{1-t_2^2} e^{i\phi_{\rho_2}} & t_2 e^{i\phi_{\tau_2}} \end{pmatrix} \begin{pmatrix} \hat{u}^\dagger \\ \hat{v}^\dagger \end{pmatrix}. \quad (4)$$

Then the input states in Eq. 1 can be written as number-state representations of the output modes (u, v, w) as follows [17]:

$$\begin{aligned} |\xi, \beta, \gamma\rangle &= e^{-\frac{1}{2}(|\beta|^2 + |\gamma|^2)} \sum_{n=0, l=0, m=0} C_n \frac{(\hat{a}^\dagger)^n (\beta \hat{b}^\dagger)^l (\gamma \hat{c}^\dagger)^m}{\sqrt{n!} l! m!} |0\rangle_a |0\rangle_b |0\rangle_c \\ &= e^{-\frac{1}{2}(|\beta|^2 + |\gamma|^2)} \sum_{n=0, l=0, m=0} C_n \frac{(q_a^u \hat{u}^\dagger + q_a^v \hat{v}^\dagger + q_a^w \hat{w}^\dagger)^n}{\sqrt{n!}} \\ &\quad \times \frac{(\beta (q_b^u \hat{u}^\dagger + q_b^v \hat{v}^\dagger + q_b^w \hat{w}^\dagger))^l (\gamma (q_c^u \hat{u}^\dagger + q_c^v \hat{v}^\dagger))^m}{l! m!} |0\rangle_u |0\rangle_v |0\rangle_w. \end{aligned} \quad (5)$$

Where q_μ^ν ($\mu = a, b, c, \nu = u, v, w$) represents the relations between the operators in the input modes $(\hat{a}^\dagger, \hat{b}^\dagger, \hat{c}^\dagger)$ and those in the output modes $(\hat{u}^\dagger, \hat{v}^\dagger, \hat{w}^\dagger)$ as follows:

$$\begin{aligned} \{q_a^u, q_a^v, q_a^w\} &= \{e^{-i(\phi_{\tau_1} + \phi_{\tau_2})} t_1 t_2, e^{-i(\phi_{\rho_2} + \phi_{\tau_1})} t_1 \sqrt{1-t_2^2}, e^{-i\phi_{\rho_1}} \sqrt{1-t_1^2}\} \\ \{q_b^u, q_b^v, q_b^w\} &= \{e^{i\phi_{\rho_1}} \sqrt{1-t_1^2} e^{-i\phi_{\tau_2}} t_2, -e^{i\phi_{\rho_1}} \sqrt{1-t_1^2} e^{-i\phi_{\rho_2}} \sqrt{1-t_2^2}, e^{i\phi_{\tau_1}} t_1\} \\ \{q_c^u, q_c^v\} &= \{-e^{i\phi_{\rho_2}} \sqrt{1-t_2^2}, e^{i\phi_{\tau_2}} t_2\}. \end{aligned} \quad (7)$$

Using the trinomial coefficients, $|\xi, \beta, \gamma\rangle$ in Eq. 8 becomes

$$\begin{aligned} |\xi, \beta, \gamma\rangle &= e^{-\frac{1}{2}(|\beta|^2 + |\gamma|^2)} \sum_{n=0, l=0, m=0} C_n \beta^l \gamma^m \frac{\sqrt{n!}}{n_u! n_v! n_w!} \frac{1}{l_u! l_v! l_w!} \frac{1}{m_u! m_v!} \\ &\quad \times (q_a^u)^{n_u} (q_a^v)^{n_v} (q_a^w)^{n_w} (q_b^u)^{l_u} (q_b^v)^{l_v} (q_b^w)^{l_w} (q_c^u)^{m_u} (q_c^v)^{m_v} \\ &\quad \times (\hat{u}^\dagger)^{n_u + l_u + m_u} (\hat{v}^\dagger)^{n_v + l_v + m_v} (\hat{w}^\dagger)^{n_w + l_w} |0\rangle_u |0\rangle_v |0\rangle_w, \end{aligned} \quad (8)$$

where the n' summation indicates all summations for non negative numbers n_u , n_v , and n_w such that $n_u + n_v + n_w = n$. After collecting all terms that satisfy $N_u = n_u + l_u + m_u$, $N_v = n_v + l_v + m_v$, and $N_w = n_w + l_w$ over all n, l , and m , Eq. 8 can be written with new coefficients $C(N_u, N_v, N_w)$ as follows

$$|\xi, \beta, \gamma \rangle_{uvw} = \sum_{N_u=0, N_v=0, N_w=0} C(N_u, N_v, N_w) |N_u \rangle |N_v \rangle |N_w \rangle. \quad (9)$$

If two detectors in the v and w modes simultaneously detect a single photon, the probability of finding n photons in the output mode u becomes

$$|C_s(n)|^2 \equiv |C(N_u = n, N_v = 1, N_w = 1)|^2. \quad (10)$$

III. WIGNER FUNCTION OPTIMIZATION

The probability of finding n photons in the output mode u when two detectors in the v and w modes simultaneously detect a single photon, C_s in Eq. 10, can be explicitly written as a function of the amplitudes of the three input beams, the phase differences of three beams, and the transmittances of the two beam splitters [17, 18]. In order to generate Yurke-Stoler states[19], we calculate the relative coefficients $C_s(n)/C_s(0)$ as follows

$$\left\{ \frac{C_s(1)}{C_s(0)}, \frac{C_s(2)}{C_s(0)}, \dots \right\} = \left\{ e^{i\theta} \gamma_0 \frac{2t_2^2 - 1}{\sqrt{1 - t_2^2}}, \frac{1}{\sqrt{2}} \{ e^{2i\theta} (1 - 3t_2^2) \gamma_0^2 - 3e^{i\phi} t_1^2 t_2^2 \tanh s \}, \dots \right\} \quad (11)$$

To find a simple solution, we set the amplitude of the $|\beta_0 \rangle$ to zero. Although, it's not possible to match all the coefficients, we can optimize the conditions for the generation through a numerical optimization. At first, we attempted to increase the fidelity of the tested state. The fidelity (F) between the two pure state $|s_1 \rangle$ and $|s_2 \rangle$. is defined by an overlap $|\langle s_1 | s_2 \rangle|$ such as,

$$\begin{aligned} F &= \left| \sum_{n,m} a_n^* b_m \langle n | m \rangle \right| \\ &= \left| \sum_n a_n^* b_n \right|, \end{aligned} \quad (12)$$

where we used $|s_1 \rangle = \sum_n a_n |n \rangle$ and $|s_2 \rangle = \sum_m b_m |m \rangle$.

On the other hand, the Yurke-Stoler state is very sensitive to the relative phase of each Fock state. So we calculated the Wigner function of each trial state and then minimized the absolute square of the difference between two Wigner functions of the Yurke-Stoler state

and target states. This method is more efficient than the method using the fidelity in our numerical computer algorithm.

The Wigner function of the Yurke-Stoler state W_{YS} is

$$W_{YS}(x, p, \alpha, \zeta) = \frac{1}{\pi} \int e^{2ipy} \psi_{YS}(x-y, \alpha, \zeta) \psi_{YS}^*(x+y, \alpha, \zeta) dy, \quad (13)$$

where the Yurke-Stoler state ψ_{YS} is

$$\psi_{YS}(x, \alpha, \zeta) = \langle x | (|\alpha \rangle + e^{i\zeta} |-\alpha \rangle). \quad (14)$$

For the trial function $g(x)$

$$g(x) = \sum_{n=0} C_s(n) \psi_n(x), \quad (15)$$

with $\psi_n(x) = \langle x | n \rangle$, the Wigner function of the trial functions W_g becomes

$$W_g(x, p) = \frac{1}{\pi} \int e^{2ipy} g(x-y) g^*(x+y) dy. \quad (16)$$

Then the absolute square of the difference between the two Wigner functions D_w is

$$\begin{aligned} D_w &= 2\pi \int_{x,p} |W_{YS}(x, p, \alpha, \zeta) - W_g(x, p)|^2 dp dx \\ &= 1 - 2\pi \int_{x,p} W_{YS}(x, p, \alpha, \zeta) W_g(x, p) dp dx. \end{aligned} \quad (17)$$

The second term can be expanded as follows,

$$\begin{aligned} &2\pi \int_{x,p} W_{YS}(x, p, \alpha, \zeta) \left\{ \frac{1}{\pi} \int_y e^{2ipy} g(x-y) g^*(x+y) dy \right\} dp dx \\ &= 2\pi \int_{x,p} W_{YS}(x, p, \alpha, \zeta) \left\{ \frac{1}{\pi} \int_y e^{2ipy} \sum_{n=0} C_s(n) \psi_n(x-y) \sum_{m=0} C_s^*(m) \psi_n^*(x+y) dy \right\} dp dx \\ &= 2 \sum_{n=0, m=0} C_s(n) C_s^*(m) I(n, m, \alpha, \zeta). \end{aligned} \quad (18)$$

Algebraic manipulation leads to

$$I(n, m, \alpha, \zeta) = \int_{x,p,y} e^{2ipy} W(x, p, \alpha, \zeta) \psi_n(x-y) \psi_n^*(x+y) dy dp dx \quad (19)$$

$$= \frac{\{(-1)^n + e^{i\zeta}\} \{1 + (-1)^m e^{i\zeta}\} \alpha^{n+m}}{2(1 + 2e^{2\alpha^2 + i\zeta} + e^{2i\zeta}) \pi \sqrt{n!} \sqrt{m!}} e^{\alpha^2} \quad (20)$$

Finally, the closed integral formula in Eq. 20 can be used to efficiently minimize the absolute square of the difference between the two Wigner functions D_w .

IV. HIGH PURITY CAT-SATE GENERATION.

The generation of various nonclassical photonic-states through the use of a squeezed light source and conditional measurements on a beam splitter has been extensively studied, both theoretically and experimentally. We use squeezed vacuum states, combine the addition and subtraction of photons[17]. Using the cascaded beam splitter as used by Bimbard et al. [9] (Fig. 1), we can control the probabilities of the generated quantum states. The numerical conditions necessary to generate high-purity $|1\rangle$, $|2\rangle$, and $|1\rangle + re^{i\psi}|2\rangle$ states were found with a value of more than 1000 for the expected theoretical signal-to-noise ratio [18]. The two beam splitters and two coherent beams with two detectors in the output port give us a degree of freedom to control the output, which is highly nonclassical.

We present the conditions to generate the Yurke-Stoler state with $\alpha = 1$ and $\zeta = 0, \frac{2}{3}\pi, \frac{4}{3}\pi$, in Table I. The interesting thing is that if we only change the relative phase of the input beams (ϕ , and θ), we can generate three states

$$\{|\alpha_1\rangle + |-\alpha_1\rangle, |\alpha_1\rangle + e^{i\frac{2}{3}\pi}|-\alpha_1\rangle, |\alpha_1\rangle + e^{i\frac{4}{3}\pi}|-\alpha_1\rangle\}, \quad (21)$$

where $\alpha_1 = 1$. The Yurke-Stoler state $|\alpha_1\rangle + |-\alpha_1\rangle$ can also be generated by blocking the $|\gamma_0 e^{i\zeta}\rangle$ state and setting the phase differences. The phase differences seem meaningless if the two coherent beams are removed, but the actual phase differences contains all the phases of beam splitters ($\phi_{\rho_1}, \phi_{\rho_2}, \phi_{\tau_1}, \phi_{\tau_2}$) [17]. Therefore the phase differences should be controlled and checked through the very weak coherent light inputs in the actual experiments. The fidelity of the three Yurke-Stoler states are greater than 0.995, and the absolute difference of the Wigner states is of less than 0.01.

With fixed amplitudes for the input states and the transmittances of the two beam splitters, we obtain similar quantum states according to the relative phases of the two beams. The last column in Table I, $\text{Log}(P)$, shows the logarithmic value of the generating probability. The meaning of the probability is that, for a condition where the amplitudes of the input beams and the fixed transmittance value are given, there is a chance to simultaneously detect a pair of single photons at each detector. If we consider the train of the input pulses, there is approximately 1 chance to generate a state ($|\alpha_1\rangle + e^{i\frac{2}{3}\pi}|-\alpha_1\rangle$) with a fidelity of 0.997 for every 1950 pulses.

In Fig. 2 (a), we plotted the Wigner function of the generated state by using the numerical parameters in Table I. The Wigner functions is calculated for the state with $\zeta = \frac{4}{3}\pi$. In Fig.

TABLE I: ($|\alpha_1 \rangle + e^{i\zeta} |-\alpha_1 \rangle$)-state generating conditions.

ζ	s	γ_0	t_1	t_2	ϕ	θ	F	$\text{Log}(D_w)$	$\text{Log}(P)$
0	$\frac{1}{2}$	0.0	0.797	0.997	π	0	0.995	-2.02	-3.29
$\frac{2}{3}\pi$	$\frac{1}{2}$	0.137	0.797	0.997	π	$-\frac{1}{2}\pi$	0.997	-2.29	-3.29
$\frac{4}{3}\pi$	$\frac{1}{2}$	0.137	0.797	0.997	$-\pi$	$\frac{1}{2}\pi$	0.997	-2.23	-3.29

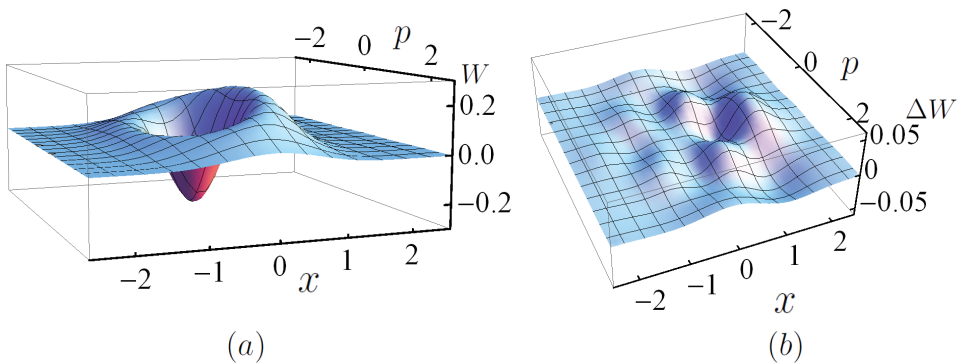


FIG. 2: (a) Wigner function of the generated states ($\zeta = \frac{4}{3}\pi$) under the setup in Table I. (b) Difference of the Wigner function between the state in (a) and the Yurks-Stoler state ($|\alpha_1 \rangle + e^{i\frac{4}{3}\pi} |-\alpha_1 \rangle$).

2 (b), we plotted the difference between the two Wigner functions for the state in Fig. 2 (a) and the theoretical Yurks-Stoler state ($|\alpha_1 \rangle + e^{i\frac{4}{3}\pi} |-\alpha_1 \rangle$).

The generation scheme in Table I does not use a coherent beam ($|\beta_0 \rangle$). If we add a coherent beam ($|\beta_0 \rangle$), we can have precise control over the generated state, and then we can increase the purity of that state. We have already found the generating condition for several Fock states with a signal-to-noise ratio higher than 1000 [18]. Similarly, if we unblock

TABLE II: even-cat-state ($|\alpha \rangle + |-\alpha \rangle$) generating conditions.

α	s	β_0	γ_0	t_1	t_2	ϕ	θ	$1 - F$	$\text{Log}(D_w)$	$\text{Log}(p)$
1	0.500	0.341	0.212	0.832	0.745	$-\pi$	$-\pi$	5.1×10^{-5}	-3.99	-2.36
$\frac{1}{\sqrt{2}}$	0.455	0.392	0.181	0.779	0.593	π	$-\pi$	1.2×10^{-6}	-5.62	-2.32
$\sqrt{2}$	0.489	0.208	0.178	0.930	0.919	$-\pi$	$-\pi$	1.2×10^{-3}	-2.63	-2.75

the b port in the experimental set up in Fig. 1, we can increase the fidelity and decrease the absolute square of the differences of the two Wigner functions.

We find the generating condition for the Yurke-Stoler state with $\zeta = 0$, which is also known as the even-cat-state in Table II. For the even-cat-state with $\alpha = 1$, the fidelity is greater than 0.9999, and the absolute square of the difference between the two Wigner state of the generated state and the theoretical state (D_w) is less than 1.02×10^{-4} .

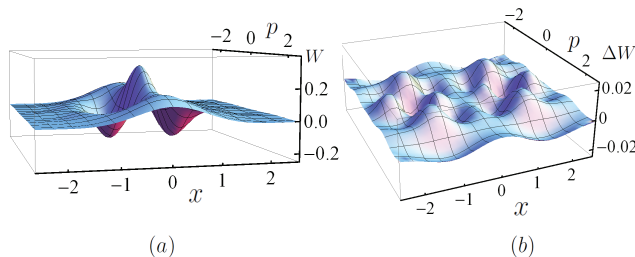


FIG. 3: (a) Wigner function of the generated states ($\alpha = \sqrt{2}$) under the setups in Table II. (b) Difference of the Wigner function between the state in (a) and the even-cat-state ($|\sqrt{2} \rangle + |-\sqrt{2} \rangle$)

The difference between two Wigner functions is much smaller than 2.4×10^{-6} for the even-cat-state with $\alpha = \frac{1}{\sqrt{2}}$, and the $1 - F$ becomes 1.2×10^{-6} . Although, it is easy to generate the even-cat-state for the smaller value of α , the estimated purity of the even-cat-state especially high. For the even-cat-state with $\alpha = \sqrt{2}$, the estimated D_w is about 2.32×10^{-3} , and the $1 - F$ becomes 1.2×10^{-3} . In Fig. 3 (a), we plotted the Wigner function

TABLE III: odd-cat-state ($|\alpha > -| - \alpha >$) generating conditions.

α	s	β_0	γ_0	t_1	t_2	ϕ	θ	$1 - F$	$\text{Log}(D_w)$	$\text{Log}(P)$
1	0.500	0.723	0.012	0.946	0.921	$-\pi$	0	1.3×10^{-3}	- 2.58	-2.29
$\frac{1}{\sqrt{2}}$	0.325	0.117	0.565	0.807	0.937	$-\pi$	$-\pi$	1.0×10^{-4}	-3.68	-2.44
$\sqrt{2}$	0.910	0.957	0.015	0.938	0.983	π	0	1.0×10^{-2}	-1.70	-2.42

of the generated state with $\alpha = \sqrt{2}$ by the numerical parameters in Table II. We plotted the difference between two Wigner functions for the state in Fig. 3 (a) and the theoretical even-cat-state ($|\sqrt{2} > +| - \sqrt{2} >$).

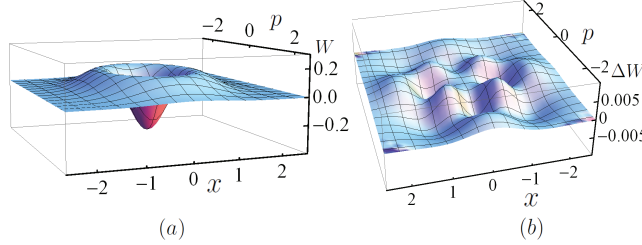


FIG. 4: (a) Wigner function of the generated states ($\alpha = \frac{1}{\sqrt{2}}$) under the setups in Table III. (b) Difference of the Wigner function between the state in (a) and the odd-cat-state ($|\frac{1}{\sqrt{2}} > -| - \frac{1}{\sqrt{2}} >$).

In our quantum state generating scheme, we also find the generating condition for the Yurke-Stoler state with $\zeta = \pi$, which is also known as the odd-cat-state seen in Table III. For the odd-cat-state with $\alpha = 1$, the fidelity is greater than 0.9987. Although, the generating probability ($\text{Log}(P)$) is almost same, the fidelity of the generated odd-cat-state is relatively lower than that of the generated even-cat-state.

In Fig. 4 (a), we plotted the Wigner function of the generated state ($\alpha = \frac{1}{\sqrt{2}}$) by using the numerical parameters in Table III, and we plotted the difference between the two Wigner functions for the state in Fig. 4 (a) and the theoretical odd-cat-state ($|\frac{1}{\sqrt{2}} > -| - \frac{1}{\sqrt{2}} >$).

The absolute square of the difference between the two Wigner states of the generated state and the theoretical state (D_w) is of less than 2.59×10^{-3} and $1 - F$ becomes 1.3×10^{-3} . Furthermore, the difference is much smaller than 2.08×10^{-4} for the odd-cat-state with $\alpha = \frac{1}{\sqrt{2}}$ and $1 - F$ becomes 1.0×10^{-4} . For the odd-cat-state with $\alpha = \sqrt{2}$, the estimated D_w is of about 2.0×10^{-2} .

V. DISCUSSION

With the explicit form, the probability amplitude for an output state is a function of the transmittance of two beam splitters and the amplitudes and relative phases of the three input beams. The probabilities are calculated when the two detectors simultaneously detect a single photon. We have included all of the coefficients of the input beams from zero to nine of the number representations for three input states.

Without a coherent state $|\beta\rangle$, it is possible to generate several Yurke-Stoler states ($|\alpha\rangle + e^{i\zeta}|\alpha\rangle$). However, considering the signal-to-noise ratio, we found that $|\beta\rangle$ increases the fidelity up to $1 - 5.1 \times 10^{-5}$ for the even-cat-state where $\alpha = 1$, and the fidelity can increase to up to 0.999999 for the even-cat-state with $\alpha = \frac{1}{\sqrt{2}}$. Even though the fidelity can decrease in the actual experiments, the possibility to generate a high-fidelity quantum state is important in quantum information science. Furthermore, if we can generate a high fidelity small cat-state, the state can be amplified through homodyne heralding [24].

Since the probabilities have complex forms, we attempted to find conditions to generate high-purity states through a numerical minimization method for the difference of the Wigner functions. In an actual experiment, s was obtained as 0.63[12], so we tried to limit the s values to 1. Considering the two coherent states $|\beta\rangle$ and $|\gamma\rangle$, the amplitudes can have large values in an actual experimental setup, but we tried to keep the amplitude to a small number.

Our calculations are based on the assumption that we have photon-resolving photo detectors, and that we can describe our system within six photon states for each input state. So, we tried to keep the amplitudes β_0 and γ_0 as small numbers in order to ensure the reliability of our assumptions. If the amplitudes are sufficiently small, we don't need photon-resolving photo detectors.

Considering the applicability to actual experiments [25], if we use the input beam as a

pulsed light with a repetition rate of 100MHz, then the generation probability of 10^{-3} results in 10^6 signals per second. In actual experiments, a high signal-to-noise ratio can be reduced as a result of experimental imperfections, such as mode matching and non-unity quantum efficiency. We assumed perfect temporal and spatial mode matching among the three input beams. These assumptions also guaranteed for the spatial and temporal mode properties of the cat states generated in our scheme to be well defined by the input states, and we can precisely control the modes of the two coherent states and the squeezed vacuum by adjusting the pump beam used to produce squeezed states. We expect high-purity spatial and temporal modes of the cat state.

A high-quality cat-state can be used to study the quantum nature of the world, and it is a key element in quantum technology.

Acknowledgments

This study was supported by the Basic Science Research Program, through the National Research Foundation of Korea (NRF), funded by the Ministry of Education, Science and Technology (20110004651)

-
- [1] M.S. Kim, J. Phys. B: At. Mol. Opt. Phys. **41**, 133001 (2008)
 - [2] F. Dell'Anno, S. De Siena, and F. Illuminati, Phys. Rep. **428**, 53 (2006).
 - [3] Shuai Wang, Hong-yi Fan, and Li-yun Hu, J. Opt. Soc. Am. B **29** 1020 (2012)
 - [4] K. J. Resch, J. S. Lundeen, and A. M. Steinberg, Phys. Rev. Lett. **88**, 113601 (2002)
 - [5] A. I. Lvovsky, H. Hansen, T. Aichele, O. Benson, J. Mlynek, and S. Schiller, Phys. Rev. Lett. **87**, 050402 (2001)
 - [6] A. Ourjoumtsev, R. Tualle-Brouiri, Ph. Grangier, Phys. Rev. Lett. **96**, 213601(2006).
 - [7] A. I. Lvovsky, and S. A. Babichev, Phys. Rev. A **66**, 011801 (2002).
 - [8] A. Zavatta, S. Viciani, and M. Bellini, Science **306**, 660 (2004).
 - [9] E. Bimbard, N. Jain, Andrew MacRae, and A. I. Lvovsky, "Quantum-optical state engineering up to the two-photon level", Nature Photonics **4**, 243 (2010).
 - [10] M. Dakna, T. Anhut, T. Opatrny, L. Kno, and D.-G. Welsch Phys. Rev. A. **55** 3184 (1997)

- [11] J. Fiurasek, R. Či Patron, and N. J. Cerf, Phys. Rev. A. **72**, 033822 (2005)
- [12] A. Ourjoumtsev, R. Tualle-Brouiri, J. Laurat, and Ph. Grangier, Science **312**, 83 (2006)
- [13] J. S. N. Nielsen, B. M. Nielsen, C. Hettich, K. Molmer, and E. S. Polzik, Phys. Rev. Lett. **97**, 083604 (2006).
- [14] K. Wakui, H. Takahashi, A. Furusawa, M. Sasaki, Opt, Exp. bf 15 3568 (2007)
- [15] A. I. Lvovsky, and J. Mylnek, Phys. Rev. Lett. **88**, 250401 (2002)
- [16] T. Gerrits, S. Glancy, T. S. Clement, B. Calkins, A. E. Lita, A. J. Miller, A. L. Migdall, S. W. Nam, R. P. Mirin, and E. Knill, Phys. Rev. A **82**, 031802 (2010)
- [17] S. H. Youn, "Engineering vacuum-evacuated photonic states with three input beams and two detectors," J. Kor. Phys. Soc. **63**, 1559 (2013).
- [18] S. H. Youn, "Conditional Generation Scheme for a High-purity Superposed State of Single and Two-photon States by Mixing Two Coherent Beams with Squeezed Vacuum States", J. Kor. Phys. Soc. Accepted (2014).
- [19] B. Yurke and D. Stoler, "Generating quantum mechanical superpositions of macroscopically distinguishable states via amplitude dispersion", Phys. Rev. Lett. **57**, 13 (1986).
- [20] L. C G Govia, E. J Pritchett, and F. Wilhelm, "Generating nonclassical states from classical radiation by subtraction measurements ", New J. Phys. **16**, 045011 (2014).
- [21] J. Zhang, W. Xiong, S. Zhang, Y. Li, and M. Feng, "Generating th Schrodinger cat states in a nanomechanical resonator coupled to a charge qubit", arXiv:1405.3129v1 [cond-mat.mes-hall] 13 May (2014).
- [22] R. Loudon, *The Quantum Theory of Light (3rd ed.)*, Oxford Univ. Press, New York (2000).
- [23] R. A. Campos, B. E. A. Saleh, and M. C. Teich, Phys. Rev. A. **40**, 1371 (1989).
- [24] A. Laghaout, J. S. Neergaard-Nielsen, I. Rigas, C. Kragh, A. Tipsmark, and U. Andersen, "Amplification of realistic Schrodinger-cat-state-like states by homodyne heralding", Phys. Rev. A **87**, 043826 (2013)
- [25] R. Dong, A. Tipsmark, A. Laghaout, L. A. Krivitsky, M. Jezek, and U. L. Andersen, "Generation of picosecond pulsed coherent state superpositions", J. Opt. Soc. Am. B, **31**, 1192 (2014)